ACS Photonics
pubs.acs.org/journal/apchd5
Perspective

MXenes for Photonics

Danzhen Zhang, Deesha Shah, Alexandra Boltasseva,* and Yury Gogotsi*

Cite This: *ACS Photonics* 2022, 9, 1108−1116
Read Online

ABSTRACT: The diverse family of two-dimensional (2D) carbides, nitrides, and carbonitrides of early transition metals called "MXenes" has been quickly growing, exhibiting excellent optical, electronic, and mechanical properties. Recently, many attractive characteristics of MXenes have been demonstrated, including plasmonic behavior, optical nonlinearities, and highly efficient photothermal conversion, enabling their successful utilization in a variety of optical and optoelectronic devices. In this article, we provide an overview of selected optical phenomena and related device applications of MXenes, such as plasmonics, photothermal effects, ultrafast optics, and nonlinear optics. We also provide a perspective on future research directions for realizing the full potential of MXenes for photonic applications. With the versatility of available compositions and their exceptional optical properties, MXenes have the potential to facilitate development of many novel tunable nanophotonic devices.

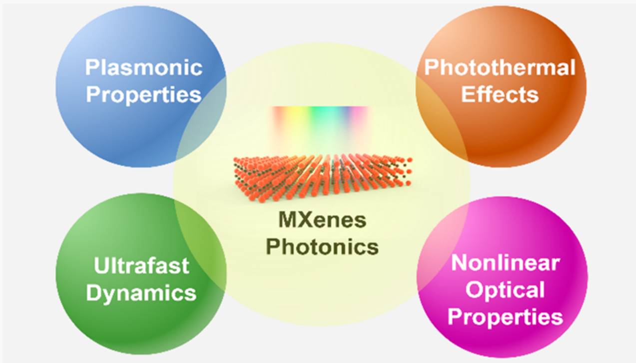

KEYWORDS: *MXenes, two-dimensional materials, photonics, plasmonics, optical properties*

■ INTRODUCTION

The discovery of graphene has resulted in the emergence of a plethora of two-dimensional (2D) materials that exhibit unique electrical and optical properties, enabling new atomically thin devices for energy storage, electronic, and photonic applications.[1−4] In 2011, Naguib et al. reported the first synthesis of Ti_3C_2 nanosheets, introducing a new family of 2D materials known as MXenes to the world.[5] In contrast to the majority of 2D materials, which are typically semiconductors or insulators, MXenes have very high carrier concentrations comparable to bulk metals, expanding the realm of applications for 2D materials.[6,7] The discovery of MXenes led to the exploration of a novel class of 2D materials with high but tunable metallic conductivity, chemical stability, and mechanical robustness. MXenes have the general chemical formula $M_{n+1}X_nT_x$, where M represents an early transition metal, X is carbon or nitrogen, n = 1−4, and T stands for surface terminations (Figure 1). One can look at them as 2 to 5 layers of transition metals, such as Ti, Nb, V, etc., bonded by 1−4 layers of carbon and/or nitrogen and terminated by OH, O, F, and other halogens or chalcogens. Since carbides are much better studied than nitrides or carbonitrides, this Perspective will focus on carbide MXenes. Typically, MXenes are synthesized by a top-down method starting with a MAX (layered carbides and nitrides with general formula $M_{n+1}AX_n$, where M represents an early transition metal, A is usually Al or Si, X is carbon or nitrogen, n = 1−4) phase or another layered precursor, followed by selective etching of the A element from the MAX phase.[8] Meanwhile, bottom-up methods, such as chemical vapor deposition, have also been utilized to synthesize ultrathin high-quality MXene crystals, such as Mo_2C.[9] With the advancement in processing techniques and a variety of existing MAX phases, the family of MXenes has been quickly expanding.

With over 30 stoichiometric varieties of MXenes reported and multiple solid solutions and high-entropy compositions, the diverse family of MXenes provides unprecedented tunability of compositions and properties, and a wide range of optical phenomena (Figure 2). On the basis of their versatile surface groups and high conductivity, various promising applications with MXenes have been demonstrated including energy storage,[10] electromagnetic interference shielding,[11] electrocatalysis,[12] and optoelectronics.[13] Moreover, due to their exceptional optical properties and unique tunability, MXenes are an extremely attractive material platform for realizing numerous novel photonic devices ranging from saturable absorbers for ultrafast lasers to surface enhanced Raman spectroscopy (SERS) substrates. Here, we discuss the recent progress in implementing MXenes for photonic

Received: January 6, 2022
Revised: February 26, 2022
Accepted: March 1, 2022
Published: March 10, 2022

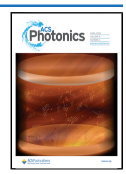

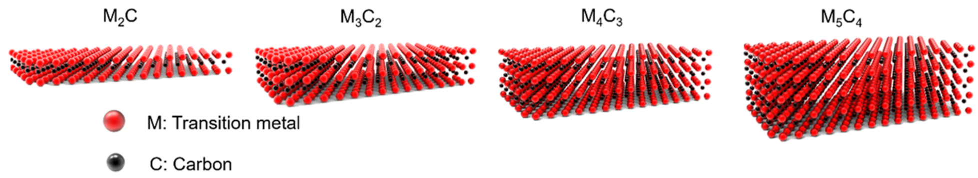

Figure 1. Schematic illustration of MXenes structure. Carbide MXenes with 3, 5, 7, and 9 atomic layers are represented as M_2C, M_3C_2, M_4C_3, and M_5C_4, respectively, where M is transition metal, C is carbon. Surface terminations are not shown.

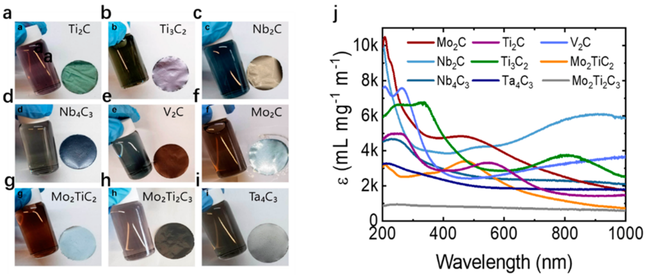

Figure 2. Optical properties of representative MXenes in the UV−vis−NIR range. (a−i) Digital photographs of MXene colloidal dispersions (20 mL) and corresponding free-standing films fabricated by vacuum filtration for (a) Ti_2C, (b) Ti_3C_2, (c) Nb_2C, (d) Nb_4C_3, (e) V_2C, (f) Mo_2C, (g) Mo_2TiC_2, (h) $Mo_2Ti_2C_3$, and (i) Ta_4C_3. Qualitative description of colors in solution/films, respectively, as follows. Ti_2C: dark purple/green; Ti_3C_2: forest green/dark purple; Nb_2C: blue/golden yellow; Nb_4C_3: gray-brown/gray-black; V_2C: green-blue/bronze; Mo_2C: brown/silver; Mo_2TiC_2: orange-brown/light blue-silver; $Mo_2Ti_2C_3$: gray/dark green-gray; and Ta_4C_3: brown/silver-gray. All MXene solutions are dispersed in deionized water with concentrations ranging between 0.01−0.05 mg mL^{-1}. The MXene film diameters are 4 cm. (j) UV−vis−NIR optical extinction properties of 2D transition metal carbides. Wavelength-dependent extinction coefficient for each MXene calculated by determining the extinction coefficient at each wavelength from 200 to 1000 nm ($h\nu$ = 6.2−1.2 eV). Reproduced with permission.[19] Copyright 2020, Wiley-VCH.

applications, including plasmonic devices, photothermal effects, and ultrafast and nonlinear optics. Finally, we provide an outlook for challenges and approaches regarding future research to further explore the optical properties and applications of MXenes.

■ PLASMONIC PROPERTIES

While noble metals have long been the primary choice for plasmonics,[14] plasmonic materials like transition metal nitrides and transparent conducting oxides exhibit great tunability and mechanical durability unlike noble metals.[15,16] Similarly, stable and robust MXenes, which are known to have high carrier concentrations as well as highly tunable optical properties (Figure 3), have gained strong interest for easy-to-fabricate plasmonic devices. The most commonly studied MXene, $Ti_3C_2T_x$, exhibits intense surface plasmons (SPs) at energies as low as 0.3 eV.[17] As shown in Figure 3a, electron energy loss spectroscopy (EELS) investigation of local surface plasmon modes of $Ti_3C_2T_x$ identified six distinct features at 0.44, 0.66, 0.8, 0.95, 1.7, and 3.5 eV.[18] The one at 1.7 eV was attributed to a transverse SP mode, and the 3.5 eV was assigned to an interband transition. In addition, the tunable response of the transverse SP mode was demonstrated via in situ annealing to reduce the −F surface groups. The induced desorption of −F group increases the free electron density noticeably and leads to a blue shift of the SP mode. Due to the strong, tunable SPs that can be excited in the near to mid infrared range, MXenes are promising candidates for plasmonic applications.

Chaudhuri et al. provided the first demonstration of an MXene based plasmonic broadband absorber by taking advantage of the large intrinsic optical absorption and localized surface plasmon resonances of nanostructured $Ti_3C_2T_x$. The $Ti_3C_2T_x$ nanodisk array fabricated on Au/Al_2O_3 showed a high absorption (85−90%) over a broad wavelength range from 400−1550 nm as shown in Figure 3b.[20] A polarization- and angle-independent broadband plasmonic absorber has also been fabricated by randomly distributing Au nanoparticles on a MXene/PMMA film.[21] The easy to fabricate metal−insulator−metal structure showed 99% absorption in the wavelength range of 300−1800 nm. These initial demonstrations of highly broadband plasmonic absorbers with MXenes opens a new door for future applications such as energy harvesting for photovoltaic devices and photothermal conversion.

Owing to the strong tunability of their SPs and hydrophilic, negatively charged surfaces, MXenes have also found applications as SERS substrates with enhancement factors (EF) of up to 10^6. Spray-coated $Ti_3C_2T_x$ demonstrated a significant increase in the EF for detecting Rhodamine 6G with a concentration of 10^{-7} M, caused by the physisorption of the dye molecules on the MXene surface (Figure 3c).[22] Experimental and numerical calculations for the thickness-dependent SERS revealed that the EF increases in thicker films due to the collective SERS enhancement in all of the individual layers of $Ti_3C_2T_x$ dominated by charge transfer (Figure 3d).[23] By combining both electromagnetic and chemical enhancement mechanisms, remarkable Raman signal enhancement can be achieved with MXenes. $Ti_3C_2T_x$ is just one material in the growing MXenes family along with Nb_2C and Ta_2C, which also exhibit remarkable SERS performance.[24] As synthesis processes mature and more MXenes are experimentally realized, further improvements in using MXenes as SERS substrates is expected through careful control and tuning of the material properties. Considering the large number of compositions and properties possible, MXenes show tremendous potential as SERS substrates for biomedical imaging and high-sensitivity environmental analysis.

With their high transmissivity and conductivity, MXenes have emerged as a promising candidate for transparent electrodes of photodetectors. Additionally, the SPs supported by MXenes can enlarge the photocurrent via SP assisted hot electron generation. Photodetectors fabricated from four different MXenes, Mo_2CT_x, $Ti_3C_2T_x$, Ti_2CT_x, and V_2CT_x, were investigated, with Mo_2CT_x showing the best performance.[25] The Mo_2CT_x photodetector exhibited a broadband efficient photocurrent in the visible range (400−800 nm), as shown in Figure 3e. Under 660 nm laser illumination, Mo_2CT_x achieved a large photoresponsivity of 9 A W^{-1} due to the transversal SP mode at 2.45 eV that enhances the photocurrent generation at visible wavelengths. Mo_2CT_x thin films also

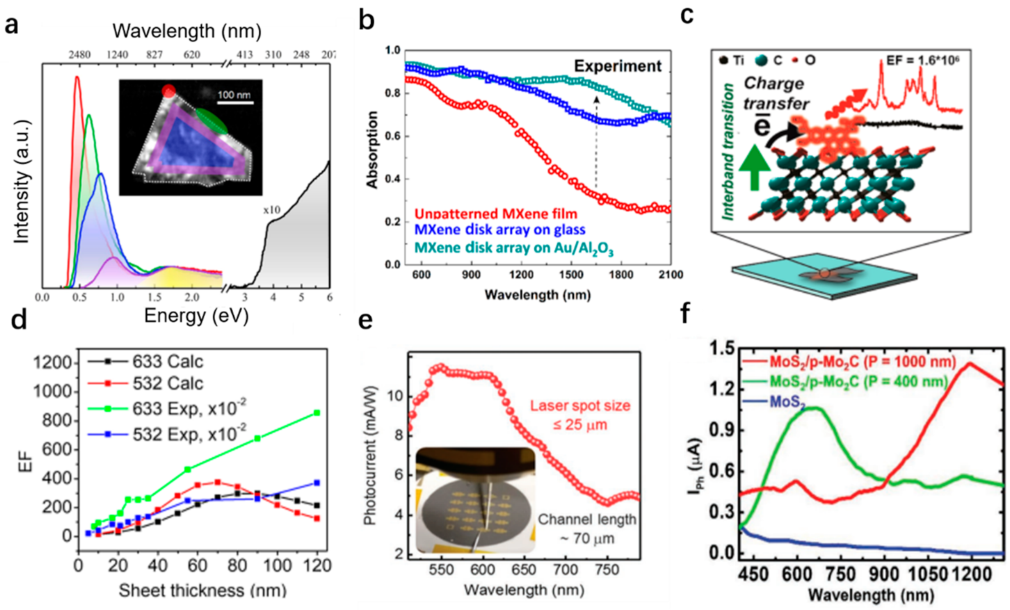

Figure 3. Plasmonic properties and applications of MXenes. (a) EELS analysis of a nanoflake of $Ti_3C_2T_x$. Reproduced with permission.[18] Copyright 2018, American Chemical Society. (b) Improvement of absorption spectra of patterned $Ti_3C_2T_x$ film. Reproduced with permission.[20] Copyright 2018, American Chemical Society. (c) A schematic of SERS substrate made from $Ti_3C_2T_x$. Reproduced with permission.[22] Copyright 2017, American Chemical Society. (d) Raman EF contributed by $Ti_3C_2T_x$ vs thickness for 532 and 633 lasers. Reproduced with permission.[23] Copyright 2020, American Chemical Society. (e) Wavelength-dependent photoresponse of Mo_2CT_x films. Reproduced with permission.[25] Copyright 2019, Wiley-VCH. (f) Spectral photocurrent curves from MoS_2 photodetector devices with and without MXene hybrid. Reproduced with permission.[26] Copyright 2019, Wiley-VCH.

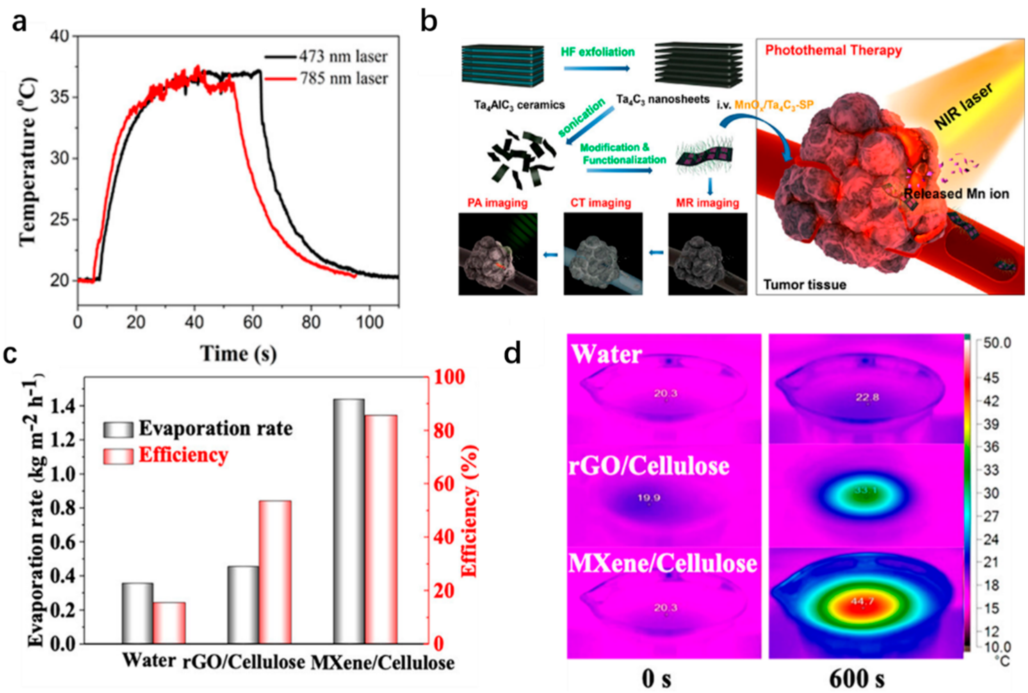

Figure 4. Photothermal properties and applications of MXenes. (a) Temperature profile of a $Ti_3C_2T_x$ droplet illuminated by different laser wavelengths. Reproduced with permission.[31] Copyright 2017, American Chemical Society. (b) Schematic of synthesis and implementation of Ta_4C_3 composite nanosheets for tumor imaging and ablation. Reproduced with permission.[39] Copyright 2017, American Chemical Society. (c) Water evaporation rates, solar steam efficiency, and (d) IR thermal images of water, MXene/cellulose, and rGO/cellulose membranes under the solar illumination of 1 sun. Reproduced with permission.[40] Copyright 2019, American Chemical Society.

showed chemical and mechanical stability, allowing successful fabrication of high-performance plasmonic photodetection devices. MXenes can also be integrated with other 2D materials such as MoS_2[26] and graphene[27] to enhance the photodetector performance. The hybrid structure of MoS_2/Mo_2CT_x has a broad spectral detection as well as high photoresponsivity larger than 10^3 A W^{-1} over 400−1300 nm (Figure 3f).[26] An InSe photodetector with plasmonic Ti_2CT_x

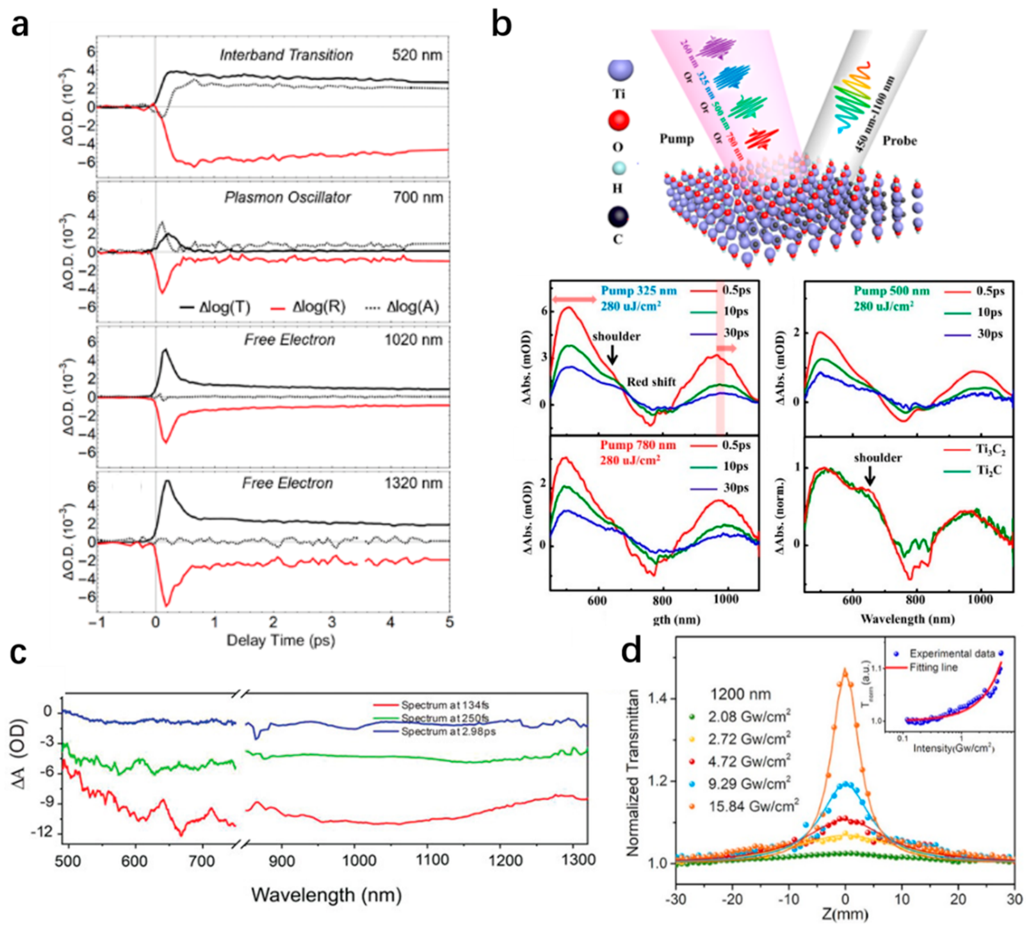

Figure 5. Ultrafast dynamics of MXenes. (a) Transmission, reflection and obtained absorption transients for 520, 700, 1020, and 1320 nm. Reproduced with permission.[41] Copyright 2020, American Chemical Society. (b) A schematic of pump−probe spectroscopy of MXenes and transient spectra under different pump excitation. Reproduced with permission.[42] Copyright 2020, American Chemical Society. (c) Ultrafast TA spectra of Nb_2CT_x. Reproduced with permission.[44] Copyright 2020, Wiley-VCH. (d) Open aperture Z-scan results of Nb_2CT_x at 1200 nm. Reproduced with permission.[45] Copyright 2020, American Chemical Society.

grating electrodes had a highly improved responsivity (10^5 A W^{-1}) and detectivity.[28] MXenes with high conductivity and intense surface plasmons can be directly used as active materials in nanophotonic devices as well as electrodes to enhance their overall performance.

■ PHOTOTHERMAL EFFECTS

Photothermal materials that efficiently convert light into thermal energy have benefitted many technologies from solar energy harvesting[29] to cancer therapy.[30] MXenes exhibit a high extinction coefficient, indicating their excellent light-to-heat conversion properties. While all possible mechanisms of interactions of MXenes with electromagnetic waves are not fully understood, the photothermal effect in metallic MXenes like $Ti_3C_2T_x$ has been attributed to SP resonances that enhance the absorption in the NIR. The internal light-to-heat conversion efficiency of $Ti_3C_2T_x$ was measured to approach 100%, while the light to water evaporation efficiency was measured to be 84%.[31] A sudden temperature rise of over 10 °C was observed in a droplet of 0.1 mg/mL $Ti_3C_2T_x$ solution as soon as a laser was shone on it, indicating immediate heat convection in the droplet (Figure 4a). Combining the plasmonic properties of silver nanoparticles and the photothermal effects of MXenes has facilitated high photothermal conversion. By hybridizing $Ti_3C_2T_x$ and silver nanoparticles in polyurethane, a wearable, healable, and transparent composite that undergoes significant temperature increases under low irradiation was developed.[32] The photothermal effect of MXenes demonstrates the possibility of MXene-based wearable heaters, heat barriers, and photothermal therapy.[33]

Leveraging the exceptional photothermal properties of MXenes has helped to advance technologies for water desalination, biomedical devices, and energy harvesting.[34−36] By combining their biocompatibility and excellent light to heat conversion, $Ti_3C_2T_x$,[37] Nb_2CT_x,[38] and $Ta_4C_3T_x$[39] and several other MXenes have been useful for biomedical applications such as photothermal cancer therapy and photoacoustic imaging (Figure 4b). Moreover, photothermal materials have attracted interest for an eco-friendly and sustainable technique to generate steam from saltwater for water purification. A flexible MXene/cellulose photothermal membrane has been developed for solar driven water purification.[40] The prepared membrane achieved an absorption of ∼94% across the UV−vis−NIR range, resulting in a surface temperature rise to 44.7 °C in 10 min. The water evaporation rate was found to be 3 times higher than that of pure water, surpassing the performance of reduced graphene oxide (Figure 4c, d). The high photothermal and water evaporation efficiency of MXenes may enable sustainable solutions for wastewater treatment.

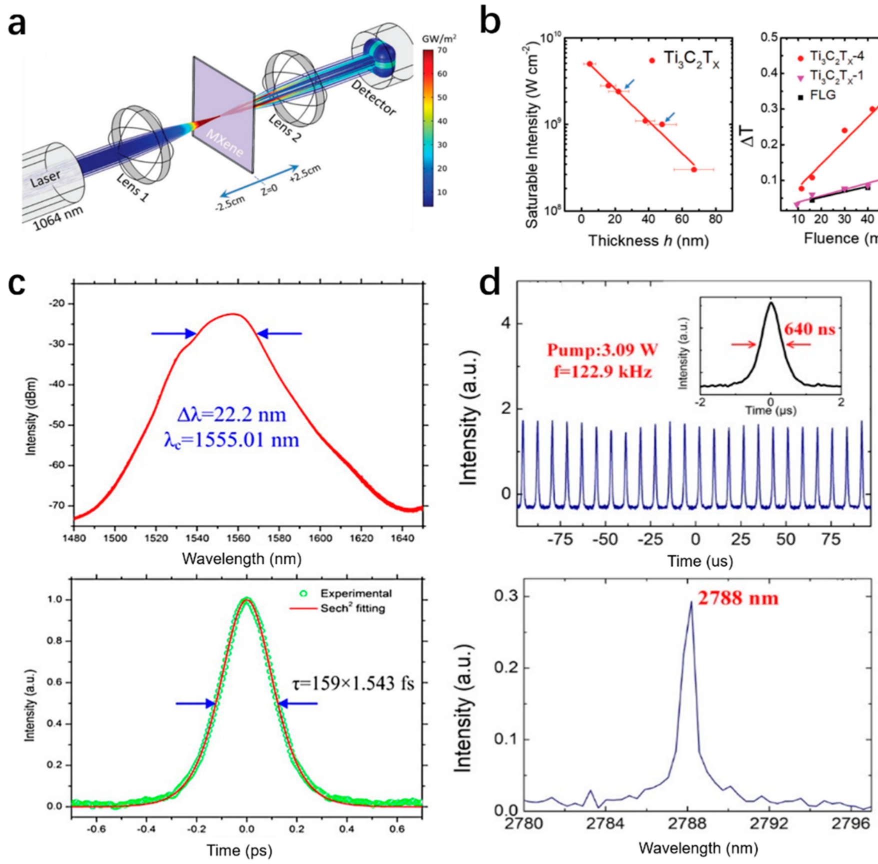

Figure 6. Nonlinear optical properties of MXenes and ultrafast lasers based on SA behavior of MXenes. (a) A schematic Z-scan measurement of MXene thin film. (b) The SA behavior of $Ti_3C_2T_x$ vs few layer graphene as a function of increasing laser energies. (a,b) Reproduced with permission.[46] Copyright 2018, Wiley-VCH. (c) Erbium-doped mode-locked fiber laser using $Ti_3C_2T_x$ saturable absorber. The laser centered at 1555 nm under power of 238 mW and the duration is estimated to be 159 fs based on the autocorrelation trace fitting. Reproduced with permission.[47] Copyright 2018, Wiley-VCH. (d) Temporal pulse trains and optical spectrum of MIR fiber laser based on $Ti_3C_2T_x$. Reproduced with permission.[51] Copyright 2020, American Chemical Society.

However, stability of MXene in water at elevated temperatures should be further increased to achieve longer operation time.

■ ULTRAFAST DYNAMICS

To better apply MXenes for a myriad of photonic and optoelectronic applications, such as laser systems, photodetection, and energy harvesting, a deep understanding of the carrier dynamics in MXenes upon photoexcitation is required. Ultrafast spectroscopy techniques have been utilized to elucidate the dynamic processes of electrons and phonons in MXenes which occur at time scales on the range of femtoseconds and picoseconds. Simultaneous ultrafast transmission and reflection (SUTR) was conducted on $Ti_3C_2T_x$ thin films with a pump laser at 785 nm to determine the temporal response of the absorption, transmission, and reflection in the wavelength ranges of 450−720 nm and 860−1350 nm.[41] Depending on the probe wavelength, the dynamics can be attributed to either interband transitions (below 600 nm), the SP resonances (800 nm), or free electrons (above 1000 nm), as shown in Figure 5a. The SUTR method allows one to determine the true transient absorption, which is conducive for advancing our understanding of optical transitions and applications of MXenes. In a separate study, the dependence of the ultrafast transient spectra on the excitation wavelength was studied using pump−probe spectroscopy (Figure 5b), with pump wavelengths of 325, 500, and 780 nm.[42] The ultrafast dynamics at the early stage were shown to be strongly dependent on the excitation and probe wavelengths and fluence. These studies on the ultrafast dynamics across a range of pump and probe wavelengths have provided a more complete picture of the underlying ultrafast processes in MXenes. Given the excellent light to heat conversion that MXenes provide, investigations on the ultrafast light-matter interactions provide an important step in successfully employing MXenes in future nanophotonic and photothermal devices.

Beyond the UV−vis−IR range, MXenes also exhibit photoinduced transient THz transparency,[43] which opens possibilities for new THz devices such as optically gated detectors and tunable EMI shielding. Moreover, $Ti_3C_2T_x$ is not the only material in the MXenes family with ultrafast electron−phonon scattering times. Nb_2CT_x also shows ultrafast cooling and recombination processes of hot carriers with a time scale less than 3 ps, as shown in Figure 5c.[44] In addition to the ultrafast dynamic properties, Nb_2CT_x exhibits higher nonlinear absorption (as showed in Figure 5d) compared to that in the visible range, and both saturable absorption and reversible saturable absorption phenomena were observed due to its unique band structure near Fermi level.[44,45] The ultrafast carrier dynamics of MXenes combined with their versatility are extremely promising for future development of ultrafast optical devices.

NONLINEAR OPTICAL PROPERTIES

When the electromagnetic field incident on a material is strong enough, the material begins to respond nonlinearly. Highly nonlinear materials are especially useful for many applications including ultrafast signal processing, ultrafast lasers, and sensing. Z-scan measurements (Figure 6a), which measure the third order nonlinearity, show that the saturable absorber behavior of $Ti_3C_2T_x$ arises from a plasmon-induced increase in the ground state absorption at 1064 nm.[46] The modulation depth and saturation fluence varies with film thickness, as shown in Figure 6b. Moreover, a large nonlinear absorption due to saturable absorption was achieved for the entire wavelength range from 800 to 1800 nm. At low pulse energies, saturable absorption results in the nonlinear response, while multiphoton absorption begins to dominate at higher pulse energies.[47] Utilizing their exceptional nonlinear optical properties, MXenes have been widely studied for applications in nonlinear photonics and ultrafast lasers.

Various ultrafast pulsed lasers based on MXene saturable absorbers have been investigated at wavelengths of 1, 1.5, 2, and 3 μm. Taking advantage of the strong saturable absorption of $Ti_3C_2T_x$, Jiang et al. fabricated an erbium-doped mode-locked fiber laser with a pulse duration of 159 fs at a wavelength of 1066 nm (Figure 6c), which is comparable to commercial Er-doped femtosecond fiber laser sources.[47] Wu et al. achieved ultrashort pulses with $Ti_3C_2T_x$ based Er-doped fiber lasers, where the pulse duration was 104 fs at 1550 nm by managing the laser cavity.[48] Other ultrafast mode-locked lasers were also achieved by using $Ti_3C_2T_x$ MXene with pulses centered at 1065.89 nm,[47] 1053.2 nm[49] and tunable broadband wavelength range from 1895 to 2050 nm.[50] Moreover, $Ti_3C_2T_x$ was used to generate ultrafast pulses in the mid infrared range centered at 2788 nm with a duration of 640 ns (Figure 6d), which is shorter than that of other 2D materials.[51] Using randomly dispersed $Ti_3C_2T_x$ flakes, coherent random lasing in the visible spectrum has also been achieved, which theoretically can be dynamically tuned due to their saturable absorption properties.[52] These studies indicate that $Ti_3C_2T_x$ MXene exhibits great potential for ultrafast photonic devices from the visible to NIR to MIR wavelength range. Beyond $Ti_3C_2T_x$ MXene, the nonlinear optical properties of other MXenes such as Ti_2CT_x were also utilized for mode-locked lasers centered at 1051, 1565, and 2800 nm.[53] The large nonlinear and linear absorption coefficient of MXenes has enabled their application in ultrafast lasers in the NIR and MIR range.

Optical properties of MXenes allow many other attractive applications, which have not been discussed in this Perspective. For example, the transverse SP resonance peaks can be shifted by 100 nm or more by applying 1 V or smaller voltage, allowing electrochromic applications of MXenes.[54] Several MXenes, like metals, have very low emission in the IR range, enabling IR stealth coatings and clothes that keep people warm in winter by minimizing radiation losses.[55,56] Optical transparency in thin films combined with high electrical conductivity and carrier mobility, and tunable work function allow the use of MXenes as transparent conductors for light-emitting diodes, solar cells and other photovoltaic devices, energy harvesting/storing windows, etc.[57,58]

CONCLUSIONS AND PERSPECTIVE

With their unique tunability of composition and properties and the various MXene structures, this large family of 2D transition metal carbides, nitrides, and carbonitrides has been investigated for a broad range of photonic devices, including plasmonics, light to heat conversion applications, and nonlinear optical devices. In this article, we have briefly described the linear and nonlinear optical properties, ultrafast carrier dynamics, and photothermal effects of MXenes. However, a deeper understanding and exploration of MXenes' optical properties is needed to realize their full potential in various photonic applications.

The current synthesis strategy for MXenes mainly focuses on top-down methods, which require the use of toxic acid etching. This etching method introduces many termination groups to the surface of MXenes such as —Cl, —F, ═O, which affects the plasmonic peaks of MXenes.[19] Thus, it is necessary to pursue more environmentally friendly and controllable synthesis methods. Chemical vapor deposition (CVD) has been investigated for the synthesis of ultrathin Mo_2C crystals with a size of 100 μm,[9] which have no termination on the surface. Other greener techniques, such as molten salt synthesis, have been reported recently to modify the surface termination groups including chlorine, selenium, and sulfur, as well as to produce bare MXenes.[59] Various synthesis methods provide additional possibilities for tuning the composition and the optical properties of MXenes. For example, although semiconducting MXenes have been predicted theoretically with direct or indirect bandgaps in many cases,[60−63] there have not been convincing experimental demonstrations for single-layer MXenes. Most measurements reported so far were done on multilayer films produced by assembly of MXene flakes. New synthesis methods to produce large single-layer flakes with controlled surface terminations are needed to measure intrinsic electronic properties and verify the bandgaps of different MXenes that have been predicted. With the achievement of tunable bandgaps, MXenes can be further applied in other optical and photonic devices such as single-photon emitting devices, excitonic LEDs, and photodetectors with drastic improvements in performance.

Despite the enormous diversity of MXenes, most optical studies have been focused on $Ti_3C_2T_x$, the first discovered, most common, and widely studied MXene. Other MXenes, such as solid-solution MXenes, have shown great potential for tuning and optimization of electrochemical properties and electromagnetic interference shielding performance.[64,65] Optical experiments on solid-solution MXenes[66,67] have demonstrated their promise for tuning the plasmonic response. For ultrafast photonics, other MXenes beyond Ti-based MXenes, such as V_2CT_x, were used to generate harmonic pulse as well.[68] On the basis of these results, there are many more MXenes worth exploring to achieve tailorable nanophotonic devices.

As a new kind of 2D plasmonic metallic material with properties tunable via the structure, composition and surface terminations, and mechanical and chemical stability, MXenes have exhibited immense potential for optics and photonics. While there are still several challenges not only in their synthesis but also in the basic understanding of MXenes, continuous efforts toward advancing material processing techniques and investigating their optical properties will shed more light on their optical properties and enable new photonic applications of MXenes.

https://doi.org/10.1021/acsphotonics.2c00040
ACS Photonics 2022, 9, 1108−1116

AUTHOR INFORMATION

Corresponding Authors

Alexandra Boltasseva − *School of Electrical and Computer Engineering and Birck Nanotechnology Center, Purdue University, West Lafayette, Indiana 47907, United States;* orcid.org/0000-0001-8905-2605; Email: aeb@purdue.edu

Yury Gogotsi − *A. J. Drexel Nanomaterials Institute, and Department of Materials Science and Engineering, Drexel University, Philadelphia, Pennsylvania 19104, United States;* orcid.org/0000-0001-9423-4032; Email: gogotsi@drexel.edu

Authors

Danzhen Zhang − *A. J. Drexel Nanomaterials Institute, and Department of Materials Science and Engineering, Drexel University, Philadelphia, Pennsylvania 19104, United States;* orcid.org/0000-0002-0005-2674

Deesha Shah − *School of Electrical and Computer Engineering and Birck Nanotechnology Center, Purdue University, West Lafayette, Indiana 47907, United States;* orcid.org/0000-0001-7001-8343

Complete contact information is available at:
https://pubs.acs.org/10.1021/acsphotonics.2c00040

Funding

D.S. and A.B. acknowledge funding from AFOSR Grant #FA9550-20-1-0124. D.Z. and Y.G. acknowledge funding from NSF Grant DMR-2041050.

Notes

The authors declare no competing financial interest.

REFERENCES

(1) Novoselov, K. S.; Geim, A. K.; Morozov, S. V.; Jiang, D.; Zhang, Y.; Dubonos, S. V.; Grigorieva, I. V.; Firsov, A. A. Electric Field Effect in Atomically Thin Carbon Films. *Science* **2004**, *306* (5696), 666−669.

(2) Fiori, G.; Bonaccorso, F.; Iannaccone, G.; Palacios, T.; Neumaier, D.; Seabaugh, A.; Banerjee, S. K.; Colombo, L. Electronics based on two-dimensional materials. *Nat. Nanotechnol.* **2014**, *9* (10), 768−79.

(3) Zhang, P.; Wang, F.; Yu, M.; Zhuang, X.; Feng, X. Two-dimensional materials for miniaturized energy storage devices: from individual devices to smart integrated systems. *Chem. Soc. Rev.* **2018**, *47* (19), 7426−7451.

(4) Basov, D. N.; Fogler, M. M.; García de Abajo, F. J. Polaritons in van der Waals materials. *Science* **2016**, *354* (6309), aag1992.

(5) Naguib, M.; Kurtoglu, M.; Presser, V.; Lu, J.; Niu, J.; Heon, M.; Hultman, L.; Gogotsi, Y.; Barsoum, M. W. Two-dimensional nanocrystals produced by exfoliation of Ti_3AlC_2. *Adv. Mater.* **2011**, *23* (37), 4248−53.

(6) VahidMohammadi, A.; Rosen, J.; Gogotsi, Y. The world of two-dimensional carbides and nitrides (MXenes). *Science* **2021**, *372* (6547), No. eabf1581.

(7) Hantanasirisakul, K.; Gogotsi, Y. Electronic and Optical Properties of 2D Transition Metal Carbides and Nitrides (MXenes). *Adv. Mater.* **2018**, *30* (52), No. e1804779.

(8) Anayee, M.; Kurra, N.; Alhabeb, M.; Seredych, M.; Hedhili, M. N.; Emwas, A. H.; Alshareef, H. N.; Anasori, B.; Gogotsi, Y. Role of acid mixtures etching on the surface chemistry and sodium ion storage in $Ti_3C_2T_x$ MXene. *Chem. Commun.* **2020**, *56* (45), 6090−6093.

(9) Xu, C.; Wang, L.; Liu, Z.; Chen, L.; Guo, J.; Kang, N.; Ma, X.-L.; Cheng, H.-M.; Ren, W. Large-area high-quality 2D ultrathin Mo_2C superconducting crystals. *Nat. Mater.* **2015**, *14*, 1135−1141.

(10) Lukatskaya, M. R.; Mashtalir, O.; Ren, C. E.; Dall'Agnese, Y.; Rozier, P.; Taberna, P. L.; Naguib, M.; Simon, P.; Barsoum, M. W.; Gogotsi, Y. Cation intercalation and high volumetric capacitance of two-dimensional titanium carbide. *Science* **2013**, *341* (6153), 1502−1505.

(11) Han, M.; Yin, X.; Hantanasirisakul, K.; Li, X.; Iqbal, A.; Hatter, C. B.; Anasori, B.; Koo, C. M.; Torita, T.; Soda, Y.; Zhang, L.; Cheng, L.; Gogotsi, Y. Anisotropic MXene Aerogels with a Mechanically Tunable Ratio of Electromagnetic Wave Reflection to Absorption. *Adv. Opt. Mater.* **2019**, *7* (10), 1900267.

(12) Seh, Z. W.; Fredrickson, K. D.; Anasori, B.; Kibsgaard, J.; Strickler, A. L.; Lukatskaya, M. R.; Gogotsi, Y.; Jaramillo, T. F.; Vojvodic, A. Two-Dimensional Molybdenum Carbide (MXene) as an Efficient Electrocatalyst for Hydrogen Evolution. *ACS Energy Lett.* **2016**, *1* (3), 589−594.

(13) Hantanasirisakul, K.; Alhabeb, M.; Lipatov, A.; Maleski, K.; Anasori, B.; Salles, P.; Ieosakulrat, C.; Pakawatpanurut, P.; Sinitskii, A.; May, S. J.; Gogotsi, Y. Effects of Synthesis and Processing on Optoelectronic Properties of Titanium Carbonitride MXene. *Chem. Mater.* **2019**, *31* (8), 2941−2951.

(14) Gramotnev, D. K.; Bozhevolnyi, S. I. Plasmonics beyond the diffraction limit. *Nat. Photonics* **2010**, *4* (2), 83−91.

(15) Naik, G. V.; Shalaev, V. M.; Boltasseva, A. Alternative plasmonic materials: beyond gold and silver. *Adv. Mater.* **2013**, *25* (24), 3264−94.

(16) Gui, L.; Bagheri, S.; Strohfeldt, N.; Hentschel, M.; Zgrabik, C. M.; Metzger, B.; Linnenbank, H.; Hu, E. L.; Giessen, H. Nonlinear Refractory Plasmonics with Titanium Nitride Nanoantennas. *Nano Lett.* **2016**, *16* (9), 5708−13.

(17) Mauchamp, V.; Bugnet, M.; Bellido, E. P.; Botton, G. A.; Moreau, P.; Magne, D.; Naguib, M.; Cabioc'h, T.; Barsoum, M. W. Enhanced and tunable surface plasmons in two-dimensional Ti_3C_2 stacks: Electronic structure versus boundary effects. *Phys. Rev. B* **2014**, *89* (23), 235428.

(18) El-Demellawi, J. K.; Lopatin, S.; Yin, J.; Mohammed, O. F.; Alshareef, H. N. Tunable Multipolar Surface Plasmons in 2D $Ti_3C_2T_x$ MXene Flakes. *ACS Nano* **2018**, *12* (8), 8485−8493.

(19) Maleski, K.; Shuck, C. E.; Fafarman, A. T.; Gogotsi, Y. The Broad Chromatic Range of Two-Dimensional Transition Metal Carbides. *Adv. Opt. Mater.* **2021**, *9* (4), 2001563.

(20) Chaudhuri, K.; Alhabeb, M.; Wang, Z.; Shalaev, V. M.; Gogotsi, Y.; Boltasseva, A. Highly Broadband Absorber Using Plasmonic Titanium Carbide (MXene). *ACS Photonics* **2018**, *5* (3), 1115−1122.

(21) Ali, W.; Mideksa, M. F.; Hou, K.; Li, H.; Wang, X.; Tang, Z. All-Solution-Processed Ultrahigh Broadband and Wide-Angle Perfect Absorber Based on MXene-Gold Nanoparticles. *Adv. Opt. Mater.* **2020**, *8* (21), 2000447.

(22) Sarycheva, A.; Makaryan, T.; Maleski, K.; Satheeshkumar, E.; Melikyan, A.; Minassian, H.; Yoshimura, M.; Gogotsi, Y. Two-Dimensional Titanium Carbide (MXene) as Surface-Enhanced Raman Scattering Substrate. *J. Phys. Chem. C* **2017**, *121* (36), 19983−19988.

(23) Limbu, T. B.; Chitara, B.; Garcia Cervantes, M. Y.; Zhou, Y.; Huang, S.; Tang, Y.; Yan, F. Unravelling the Thickness Dependence and Mechanism of Surface-Enhanced Raman Scattering on $Ti_3C_2T_x$ MXene Nanosheets. *J. Phys. Chem. C* **2020**, *124* (32), 17772−17782.

(24) Peng, Y.; Lin, C.; Long, L.; Masaki, T.; Tang, M.; Yang, L.; Liu, J.; Huang, Z.; Li, Z.; Luo, X.; Lombardi, J. R.; Yang, Y. Charge-Transfer Resonance and Electromagnetic Enhancement Synergistically Enabling MXenes with Excellent SERS Sensitivity for SARS-CoV-2 S Protein Detection. *Nano-Micro Lett.* **2021**, *13* (1), 52.

(25) Velusamy, D. B.; El-Demellawi, J. K.; El-Zohry, A. M.; Giugni, A.; Lopatin, S.; Hedhili, M. N.; Mansour, A. E.; Fabrizio, E. D.; Mohammed, O. F.; Alshareef, H. N. MXenes for Plasmonic Photodetection. *Adv. Mater.* **2019**, *31* (32), No. e1807658.

(26) Jeon, J.; Choi, H.; Choi, S.; Park, J.-H.; Lee, B. H.; Hwang, E.; Lee, S. Transition-Metal-Carbide (Mo_2C) Multiperiod Gratings for Realization of High-Sensitivity and Broad-Spectrum Photodetection. *Adv. Funct. Mater.* **2019**, *29* (48), 1905384.

(27) Kang, Z.; Zheng, Z.; Wei, H.; Zhang, Z.; Tan, X.; Xiong, L.; Zhai, T.; Gao, Y. Controlled Growth of an Mo_2C-Graphene Hybrid Film as an Electrode in Self-Powered Two-Sided Mo_2C-Graphene/$Sb_2S_{0.42}Se_{2.58}$/TiO_2 Photodetectors. *Sensors (Basel)* **2019**, *19* (5), 1099.

(28) Yang, Y.; Jeon, J.; Park, J. H.; Jeong, M. S.; Lee, B. H.; Hwang, E.; Lee, S. Plasmonic Transition Metal Carbide Electrodes for High-Performance InSe Photodetectors. *ACS Nano* **2019**, *13* (8), 8804−8810.

(29) Chen, H.; Wu, S.-L.; Wang, H.-L.; Wu, Q.-Y.; Yang, H.-C. Photothermal Devices for Sustainable Uses Beyond Desalination. *Adv. Energy Sustainability Res.* **2021**, *2* (3), 2000056.

(30) Jaque, D.; Martinez Maestro, L.; del Rosal, B.; Haro-Gonzalez, P.; Benayas, A.; Plaza, J. L.; Martin Rodriguez, E.; Garcia Sole, J. Nanoparticles for photothermal therapies. *Nanoscale* **2014**, *6* (16), 9494−530.

(31) Li, R.; Zhang, L.; Shi, L.; Wang, P. MXene Ti_3C_2: An Effective 2D Light-to-Heat Conversion Material. *ACS Nano* **2017**, *11* (4), 3752−3759.

(32) Fan, X.; Ding, Y.; Liu, Y.; Liang, J.; Chen, Y. Plasmonic $Ti_3C_2T_x$ MXene Enables Highly Efficient Photothermal Conversion for Healable and Transparent Wearable Device. *ACS Nano* **2019**, *13* (7), 8124−8134.

(33) Lin, H.; Gao, S.; Dai, C.; Chen, Y.; Shi, J. A Two-Dimensional Biodegradable Niobium Carbide (MXene) for Photothermal Tumor Eradication in NIR-I and NIR-II Biowindows. *J. Am. Chem. Soc.* **2017**, *139* (45), 16235−16247.

(34) Xu, D.; Li, Z.; Li, L.; Wang, J. Insights into the Photothermal Conversion of 2D MXene Nanomaterials: Synthesis, Mechanism, and Applications. *Adv. Funct. Mater.* **2020**, *30* (47), 2000712.

(35) Huang, Z.; Cui, X.; Li, S.; Wei, J.; Li, P.; Wang, Y.; Lee, C.-S. Two-dimensional MXene-based materials for photothermal therapy. *Nanophotonics* **2020**, *9* (8), 2233−2249.

(36) Wang, D.; Fang, Y.; Yu, W.; Wang, L.; Xie, H.; Yue, Y. Significant solar energy absorption of MXene $Ti_3C_2T_x$ nanofluids via localized surface plasmon resonance. *Sol. Energy Mater. Sol. Cells* **2021**, *220*, 110850.

(37) Liu, G.; Zou, J.; Tang, Q.; Yang, X.; Zhang, Y.; Zhang, Q.; Huang, W.; Chen, P.; Shao, J.; Dong, X. Surface Modified Ti_3C_2 MXene Nanosheets for Tumor Targeting Photothermal/Photodynamic/Chemo Synergistic Therapy. *ACS Appl. Mater. Interfaces* **2017**, *9* (46), 40077−40086.

(38) Lin, H.; Gao, S.; Dai, C.; Chen, Y.; Shi, J. A Two-Dimensional Biodegradable Niobium Carbide (MXene) for Photothermal Tumor Eradication in NIR-I and NIR-II Biowindows. *J. Am. Chem. Soc.* **2017**, *139* (45), 16235−16247.

(39) Dai, C.; Chen, Y.; Jing, X.; Xiang, L.; Yang, D.; Lin, H.; Liu, Z.; Han, X.; Wu, R. Two-Dimensional Tantalum Carbide (MXenes) Composite Nanosheets for Multiple Imaging-Guided Photothermal Tumor Ablation. *ACS Nano* **2017**, *11* (12), 12696−12712.

(40) Zha, X. J.; Zhao, X.; Pu, J. H.; Tang, L. S.; Ke, K.; Bao, R. Y.; Bai, L.; Liu, Z. Y.; Yang, M. B.; Yang, W. Flexible Anti-Biofouling MXene/Cellulose Fibrous Membrane for Sustainable Solar-Driven Water Purification. *ACS Appl. Mater. Interfaces* **2019**, *11* (40), 36589−36597.

(41) Lioi, D. B.; Stevenson, P. R.; Seymour, B. T.; Neher, G.; Schaller, R. D.; Gosztola, D. J.; Vaia, R. A.; Vernon, J. P.; Kennedy, W. J. Simultaneous Ultrafast Transmission and Reflection of Nanometer-Thick $Ti_3C_2T_x$ MXene Films in the Visible and Near-Infrared: Implications for Energy Storage, Electromagnetic Shielding, and Laser Systems. *ACS Appl. Nano Mater.* **2020**, *3* (10), 9604−9609.

(42) Zhang, Q.; Yan, L.; Yang, M.; Wu, G.; Hu, M.; Li, J.; Yuan, K.; Yang, X. Ultrafast Transient Spectra and Dynamics of MXene ($Ti_3C_2T_x$) in Response to Light Excitations of Various Wavelengths. *J. Phys. Chem. C* **2020**, *124* (11), 6441−6447.

(43) Li, G.; Amer, N.; Hafez, H. A.; Huang, S.; Turchinovich, D.; Mochalin, V. N.; Hegmann, F. A.; Titova, L. V. Dynamical Control over Terahertz Electromagnetic Interference Shielding with 2D $Ti_3C_2T_y$ MXene by Ultrafast Optical Pulses. *Nano Lett.* **2020**, *20* (1), 636−643.

(44) Gao, L.; Chen, H.; Zhang, F.; Mei, S.; Zhang, Y.; Bao, W.; Ma, C.; Yin, P.; Guo, J.; Jiang, X.; Xu, S.; Huang, W.; Feng, X.; Xu, F.; Wei, S.; Zhang, H. Ultrafast Relaxation Dynamics and Nonlinear Response of Few-Layer Niobium Carbide MXene. *Small Methods* **2020**, *4* (8), 2000250.

(45) Wang, Y.; Wang, Y.; Chen, K.; Qi, K.; Xue, T.; Zhang, H.; He, J.; Xiao, S. Niobium Carbide MXenes with Broad-Band Nonlinear Optical Response and Ultrafast Carrier Dynamics. *ACS Nano* **2020**, *14* (8), 10492−10502.

(46) Dong, Y.; Chertopalov, S.; Maleski, K.; Anasori, B.; Hu, L.; Bhattacharya, S.; Rao, A. M.; Gogotsi, Y.; Mochalin, V. N.; Podila, R. Saturable Absorption in 2D Ti_3C_2 MXene Thin Films for Passive Photonic Diodes. *Adv. Mater.* **2018**, *30* (10), 1705714.

(47) Jiang, X.; Liu, S.; Liang, W.; Luo, S.; He, Z.; Ge, Y.; Wang, H.; Cao, R.; Zhang, F.; Wen, Q.; Li, J.; Bao, Q.; Fan, D.; Zhang, H. Broadband Nonlinear Photonics in Few-Layer MXene $Ti_3C_2T_x$ (T = F, O, or OH). *Laser & Photonics Rev.* **2018**, *12* (2), 1700229.

(48) Wu, Q.; Jin, X.; Chen, S.; Jiang, X.; Hu, Y.; Jiang, Q.; Wu, L.; Li, J.; Zheng, Z.; Zhang, M.; Zhang, H. MXene-based saturable absorber for femtosecond mode-locked fiber lasers. *Opt. Express* **2019**, *27* (7), 10159−10170.

(49) Sun, X.; Zhang, B.; Yan, B.; Li, G.; Nie, H.; Yang, K.; Zhang, C.; He, J. Few-layer $Ti_3C_2T_x$ (T = O, OH, or F) saturable absorber for a femtosecond bulk laser. *Opt. Lett.* **2018**, *43* (16), 3862−3865.

(50) Ahmad, H.; Ramli, R.; Yusoff, N.; Samion, M. Z.; Ismail, M. F.; Bayang, L.; Aidit, S. N.; Zamzuri, A. K.; Thambiratnam, K. 155 nm-wideband and tunable q-switched fiber laser using an MXene $Ti_3C_2T_x$ coated microfiber based saturable absorber. *Laser Phys. Lett.* **2020**, *17* (8), 085103.

(51) Wang, Z.; Li, H.; Luo, M.; Chen, T.; Xia, X.; Chen, H.; Ma, C.; Guo, J.; He, Z.; Song, Y.; Liu, J.; Jiang, X.; Zhang, H. MXene Photonic Devices for Near-Infrared to Mid-Infrared Ultrashort Pulse Generation. *ACS Appl. Nano Mater.* **2020**, *3* (4), 3513−3522.

(52) Wang, Z.; Azzam, S. I.; Meng, X.; Alhabeb, M.; Chaudhuri, K.; Maleski, K.; Kim, Y. L.; Kildishev, A. V.; Shalaev, V. M.; Gogotsi, Y.; Boltasseva, A. Dynamically controlled random lasing with colloidal titanium carbide MXene. *Opt. Mater. Express* **2020**, *10* (9), 2304.

(53) Yi, J.; Du, L.; Li, J.; Yang, L.; Hu, L.; Huang, S.; Dong, Y.; Miao, L.; Wen, S.; Mochalin, V. N.; Zhao, C.; Rao, A. M. Unleashing the potential of Ti_2CT_x MXene as a pulse modulator for mid-infrared fiber lasers. *2D Mater.* **2019**, *6* (4), 045038.

(54) Salles, P.; Pinto, D.; Hantanasirisakul, K.; Maleski, K.; Shuck, C. E.; Gogotsi, Y. Electrochromic Effect in Titanium Carbide MXene Thin Films Produced by Dip-Coating. *Adv. Funct. Mater.* **2019**, *29* (17), 1809223.

(55) Li, L.; Shi, M.; Liu, X.; Jin, X.; Cao, Y.; Yang, Y.; Wang, W.; Wang, J. Ultrathin Titanium Carbide (MXene) Films for High-Temperature Thermal Camouflage. *Adv. Funct. Mater.* **2021**, *31* (35), 2101381.

(56) Han, M.; Zhang, D.; Shuck, C. E.; Gogotsi, Y. Ultralow and Selective Infrared Emission from MXenes. *arXiv*, May 9, 2021, 2105.04011 (accessed on May 9, 2021).

(57) Yang, L.; Dall'Agnese, C.; Dall'Agnese, Y.; Chen, G.; Gao, Y.; Sanehira, Y.; Jena, A. K.; Wang, X. F.; Gogotsi, Y.; Miyasaka, T. Surface-Modified Metallic $Ti_3C_2T_x$ MXene as Electron Transport Layer for Planar Heterojunction Perovskite Solar Cells. *Adv. Funct. Mater.* **2019**, *29* (46), 1905694.

(58) Ahn, S.; Han, T. H.; Maleski, K.; Song, J.; Kim, Y. H.; Park, M. H.; Zhou, H.; Yoo, S.; Gogotsi, Y.; Lee, T. W. A 2D Titanium Carbide MXene Flexible Electrode for High-Efficiency Light-Emitting Diodes. *Adv. Mater.* **2020**, *32* (23), No. e2000919.

(59) Kamysbayev, V.; Filatov, A. S.; Hu, H.; Rui, X.; Lagunas, F.; Wang, D.; Klie, R. F.; Talapin, D. V. Covalent surface modifications and superconductivity of two-dimensional metal carbide MXenes. *Science* **2020**, *369* (6506), 979−983.

(60) Bai, Y.; Zhou, K.; Srikanth, N.; Pang, J. H. L.; He, X.; Wang, R. Dependence of elastic and optical properties on surface terminated

groups in two-dimensional MXene monolayers: a first-principles study. *RSC Adv.* **2016**, *6* (42), 35731−35739.

(61) Zha, X.-H.; Luo, K.; Li, Q.; Huang, Q.; He, J.; Wen, X.; Du, S. Role of the surface effect on the structural, electronic and mechanical properties of the carbide MXenes. *Europhys. Lett.* **2015**, *111* (2), 26007.

(62) Liu, J.-H.; Kan, X.; Amin, B.; Gan, L.-Y.; Zhao, Y. Theoretical exploration of the potential applications of Sc-based MXenes. *Phys. Chem. Chem. Phys.* **2017**, *19* (48), 32253−32261.

(63) Yang, J.; Zhou, X.; Luo, X.; Zhang, S.; Chen, L. Tunable electronic and magnetic properties of $Cr_2M'C_2T_2$ (M′ = Ti or V; T = O, OH or F). *Appl. Phys. Lett.* **2016**, *109* (20), 203109.

(64) Wang, L.; Han, M.; Shuck, C. E.; Wang, X.; Gogotsi, Y. Adjustable electrochemical properties of solid-solution MXenes. *Nano Energy* **2021**, *88*, 106308.

(65) Han, M.; Shuck, C. E.; Rakhmanov, R.; Parchment, D.; Anasori, B.; Koo, C. M.; Friedman, G.; Gogotsi, Y. Beyond $Ti_3C_2T_x$: MXenes for Electromagnetic Interference Shielding. *ACS Nano* **2020**, *14* (4), 5008−5016.

(66) Han, M.; Maleski, K.; Shuck, C. E.; Yang, Y.; Glazar, J. T.; Foucher, A. C.; Hantanasirisakul, K.; Sarycheva, A.; Frey, N. C.; May, S. J.; Shenoy, V. B.; Stach, E. A.; Gogotsi, Y. Tailoring Electronic and Optical Properties of MXenes through Forming Solid Solutions. *J. Am. Chem. Soc.* **2020**, *142* (45), 19110−19118.

(67) Valurouthu, G.; Maleski, K.; Kurra, N.; Han, M.; Hantanasirisakul, K.; Sarycheva, A.; Gogotsi, Y. Tunable electrochromic behavior of titanium-based MXenes. *Nanoscale* **2020**, *12* (26), 14204−14212.

(68) Huang, W.; Ma, C.; Li, C.; Zhang, Y.; Hu, L.; Chen, T.; Tang, Y.; Ju, J.; Zhang, H. Highly stable MXene (V_2CT_x)-based harmonic pulse generation. *Nanophotonics* **2020**, *9* (8), 2577−2585.

https://doi.org/10.1021/acsphotonics.2c00040
ACS Photonics 2022, 9, 1108−1116